NSRRC - J04334 (2014)

Macromolecules

Article

pubs.acs.org/Macromolecules

Structure of the Electrostatic Complex of DNA with Cationic Dendrimer of Intermediate Generation: The Role of Counterion Entropy

Cheng-Che Yang,[†] Yen-Chih Huang,[‡] Chun-Yu Chen,[‡] Chun-Jen Su,[‡] Hsin-Lung Chen,[†,*] and Viktor A. Ivanov[§]

[†]Department of Chemical Engineering and Frontier Research Center on Fundamental and Applied Sciences of Matters, National Tsing Hua University, Hsin-Chu 30013, Taiwan

[‡]National Synchrotron Radiation Research Center, Hsin-Chu, Taiwan

[§]Department of Physics, Moscow State University, Moscow, Russia

Supporting Information

ABSTRACT: Polyamidoamine (PAMAM) dednrimer bearing a well-defined number of amine groups can be protonated under physiological or acidic condition to generate the macrocations capable of forming electrostatic complex (called "dendriplex") with DNA for gene delivery. Using small-angle X-ray scattering (SAXS) and small angle neutron scattering (SANS), here we constructed the morphological map of the complex of DNA with PAMAM dendrimer of generation four (G4) in terms of the dendrimer charge density and the nominal N/P ratio given by the feed molar ratio of dendrimer amine group to DNA phosphate group. With the increase of dendrimer charge density under a given nominal N/P ratio, the structure was found to transform from square columnar phase (in which the DNA chains packed in square lattice were locally straightened) to hexagonally-packed DNA superhelices (in which the DNA chains organizing in a hexagonal lattice twisted moderately into superhelices) and finally to beads-on-string structure (in which DNA wrapped around the dendrimer to form nuclesome-like array). The phase transition sequence was understood from the balance between the bending energy of DNA and the free energy of charge matching governed by the entropic gain from counterion release. Decreasing the nominal N/P ratio under fixed dendrimer charge density was found to exert the same effect as increasing dendrimer charge density; that is, the structure with higher DNA curvature tended to form at a lower nominal N/P ratio, in particular for the dendriplex with low dendrimer charge density. The effect of the N/P ratio was attributed to the tendency of the system to increase the translational entropy of the counterions released to the bulk solution by reducing the concentration of free DNA or dendrimer remained in the solution. The experimental results presented here thus demonstrated the crucial role of counterion entropy in the structural formation of DNA–dendrimer complexes, and this entropic contribution was governed by the dendrimer charge density, the nominal N/P ratio, and the initial concentrations of DNA and dendrimer used for complex preparation.

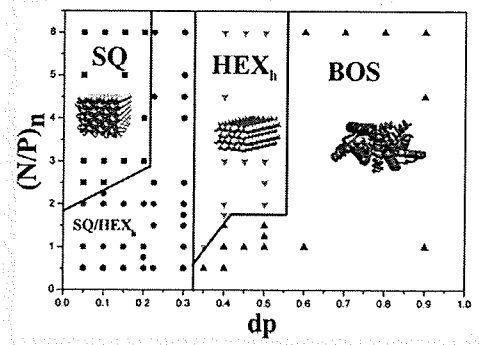

INTRODUCTION

DNA compaction has drawn significant interests due to its relevance to chromosome package in cell nucleus and nonviral gene delivery. For the delivery of extracellular DNA by nonviral vectors, the compaction of DNA is accomplished by the electrostatic complexation with synthetic compaction agents bearing positive charges. The complexation usually results in significant aggregation of DNA chains, leading to the formation of submicrometer-sized particles, which effectively protect DNA from the nuclease degradation.[1] With the excess presence of the compaction agents, the complex particles may become positively charged, which in turn facilitates their adherence to the anionic cell membranes for the subsequent endocytosis.

The compaction agents having been chosen for nonviral gene delivery include cationic lipid (liposomes), polyelectrolytes, amphiphilic block copolymers, nanoparticles, and dendrimers.[2−12] Among these materials, dendrimers have received much attention due to their immunogenicity and low cytotoxicity as well as similarity to some globule proteins in molecular geometry.[13−15] Dendrimers are a class of hyperbranched macromolecule composed of layers of monomer units irradiating from a central core. Each complete grafting cycle is called a "generation" (denoted by Gn with n being the generation number).[16] Dendrimers of low generations (e.g., G2 and G3) are floppy with loose internal structure. With increasing generation number, dendrimer molecules become more and more robust

Received: March 15, 2014
Revised: April 22, 2014
Published: April 29, 2014

 © 2014 American Chemical Society dx.doi.org/10.1021/ma500546h | Macromolecules 2014, 47, 3117−3127

and may be approximated by spherical particles with fuzzy surface and internal monomer density fluctuations.[17−22]

Poly(amidoamine) (PAMAM) dendrimers, which bear well-defined number of primary and tertiary amine groups at the surface and the interior of the molecules, respectively, represent the mostly studied dendrimer family. The amine groups in PAMAM dendrimers can be protonated conveniently under physiological or acidic condition to yield the macrocations with charge density prescribed by the pH of the aqueous solution.[23] Upon mixing with the aqueous solution of polyanionic DNA, the positively charged PAMAM dendrimer forms an electrostatic complex (called "dendriplex") with DNA spontaneously. The binding between DNA and dendrimer in the complex may give rise to special supramolecular structures characterized by their conformational, positional, and orientational order.

The gene transfection efficiency of dendriplexes was found to depend strongly on their preparation condition prescribed by the system parameters, including charge density, charge ratio and dendrimer generation.[24−26] Since these parameters may influence the structure of the dendriplex, it has been believed that the structures at different levels should play a key role governing the transfection efficiency; consequently, characterizing the dendriplex structures at different length scales and understanding their correlation with transfection efficiency are important fundamental tasks for developing effective nonviral gene vectors based on dendrimers.[24] Apart from gene delivery, the complex of DNA with dendrimer may also be considered as the synthetic model system for understanding the interaction between DNA and histone and the associated self-organization behavior of nucleosome or chromatin, considering the geometric similarity between the dendrimers of certain generations and the histone proteins.[27,28]

Several studies on the supramolecular structures of dendriplex have been reported[27,29−37] Safynia et al. were the first to disclose the mesomorphic nature of dendriplex by showing the formation of 2D hexagonal and square columnar mesophases in the complexes of DNA with cationic poly(propyleneimine) (PPI) G4 and G5 dendrimers.[31] These mesophases are characterized by the ordered packing of the locally straightened DNA chains (columns) in 2D hexagonal or square lattice, and the dendrimer molecules are accommodated in the interstitial tunnels between DNA.[31,33]

Using small-angle X-ray scattering (SAXS) and small angle neutron scattering (SANS), we have systematically investigated the nanostructures of the complexes of DNA with PAMAM dendrimers with various generations as a function of dendrimer charge density and the feed molar ratio of dendrimer amine group to DNA phosphate group (denoted as "nominal N/P ratio", $(N/P)_n$).[27,28,31,33,35] Columnar mesophases were always observed for the complexes with low-generation dendrimers (G2 and G3), with hexagonal and square columnar mesophase dominating the morphological window of G2 and G3 dendriplex, respectively.[33] In the case of the complexes with high-generation dendrimer (e.g., G9), DNA was found to consistently wrap around the dendrimer to form the "beads-on-string" structure even when the dendrimer was slightly charged.[27,28] Such a structure resembles that of the nucleosome particle formed by DNA wrapping around the histone proteins by ca. 1.7 turns.[38,39]

The observed effect of dendrimer generation number may be understood by the balance between the bending energy of DNA and the free energy of charge matching contributed by the energy of electrostatic attraction between DNA and dendrimer and the entropic gain from the release of the counterions originally condensed on DNA and dendrimer upon charge matching. Beads-on-string structure is favored for maximizing the charge matching and hence minimizes the charge matching free energy. However, DNA wrapping around dendrimer suffers high bending energy cost. For the complexes with low-generation dendrimers, the bending energy cost is too high (due to high curvature of the dendrimer molecule) to be compensated by the charge matching free energy, so that columnar mesophases in which the DNA chains are locally straightened are favored. The tendency to minimize the charge matching free energy becomes dominant at high dendrimer generation due to low dendrimer curvature; therefore, the dendriplex prefers to form beads-on-string structure to attain high degree of charge matching.

The more complicated scenario was encountered for the complexes with intermediate-generation dendrimers (e.g., G4 and G6).[31,34,35] In this case, there exists a regime of dendrimer charge density in which neither charge matching free energy nor bending energy dominates. Here the delicate balance between these two free energies may lead to the structure intermediate between the ordered columnar phase and the beads-on-string structure. For instance, we have found that, under the nominal N/P ratio of 6, DNA-PAMAM G4 dendrimer complex displayed square columnar mesophase and beads-on-string structure at low and high dendrimer charge density, respectively. A new structure called "hexagonally-packed DNA superhelices", in which DNA twisted moderately into superhelix, was identified at the intermediate charge density.[35] Recently, Dootz et al. have reported a 3D hexagonal phase for PAMAM G6 dendriplexes in which the DNA chains were proposed to adopt twist conformation.[34] These experimental observations indicated that the curvature or the tertiary structure of DNA in the dendriplex can be varied by manipulating the interplay between the charge matching free energy and DNA bending energy.

Our previous study of PAMAM G4 dendriplex focused on the effect of dendrimer charge density under a fixed nominal N/P ratio;[35] in this case, the charge density prescribed by the degree of protonation (dp, signifying the number fraction of protonated amine groups per dendrimer molecule) of the dendrimer is relevant to both the electrostatic interaction energy and the entropy gain from counterion release (as more anionic counterions can be released when the dendrimer has a higher charge density). In the present study, we expand the parameter space by investigating the effect of the nominal N/P ratio on dendriplex structure under fixed dp values. We believe that understanding the influence of such a parameter would allow us to resolve the significance of counterion entropy in the structural formation. We will demonstrate here that, at low to intermediate dendrimer charge density, $(N/P)_n$ affected the dendriplex structure obviously, where decreasing $(N/P)_n$ under a fixed denrimer dp exerted the same effect as increasing dp value under a given $(N/P)_n$. The $(N/P)_n$ effect can be understood from the tendency of the system to attain high translational entropy of the counterions once they are released to the bulk solution.

EXPERIMENTAL SECTION

Complex Preparation. All dendriplexes were prepared at room temperature (ca. 25 °C). PAMAM G4 dendrimers with different average degrees of protonation were prepared by adding predetermined amounts of 0.1 N HCl into the aqueous solutions. The dp value of the dendrimer was controlled by the amount of HCl added and it was further confirmed by pH measurement (see Supporting Information). The complex was prepared by adding the solution of the protonated dendrimer dropwise into the aqueous solution of DNA according to the prescribed nominal N/P ratio. The complexation was usually manifested

dx.doi.org/10.1021/ma500546h | Macromolecules 2014, 47, 3117−3127

by appearance of relatively cloudy suspension. The concentrations of the DNA aqueous solutions used to prepare the dendroplexes were 2, 0.5, 0.1, and 0.05 mg/mL. The dendriplexes were allowed to equilibrate at room temperature for 72 h before structural characterization. The structures of the dendriplexes did not undergo further changes with longer equilibration time.

SAXS Measurements. The structures of the dendriplexes suspended in water were probed by SAXS at room temperature. The dendriplex suspension was sealed directly into the sample cell with two Kapton windows. The SAXS measurements were performed using Beamline BL23A at the National Synchrotron Radiation Research Center (NSRRC), Hsin-Chu, Taiwan. The wavelength (λ) of the X-ray was 1.33 Å and a two-dimensional MarCCD detector with 1024 × 1024 pixel resolution was used to collect the scattering intensity data. The intensity profile was output as the plot of the scattering intensity (I) vs the scattering vector, $q = 4\pi/\lambda[\sin(\theta/2)]$ (θ = scattering angle).

SANS Measurement. The SANS measurements were conducted with the spallation neutron source at extended Q-range small angle neutron scattering (EQ-SANS) located at Beamline 6, Oak Ridge National Laboratory, Oak Ridge, TN. The instrument was operated in 60 Hz frame-skipping mode with a wavelength, λ, of 5 Å. The scattering intensity was collected with the sample-to-detector distances of 1.5 and 3 m, which yielded the SANS profile over the q range of 0.01−3.7 nm^{-1}. The measured intensity was corrected for detector sensitivity and the scattering contribution from the water solvent and empty cells.

RESULTS

The two key parameters examined here are the denerimer dp value and the nominal N/P ratio. SAXS and SANS were employed to reveal the structures of the dendriplexes. It has been shown previously that SAXS intensity of the dendriplex suspended in water (H_2O or D_2O) is dominated by DNA component because the X-ray scattering length density (SLD) contrast of DNA is about 2.85 times that of dendrimer.[27] On the other hand, the SANS intensity of the dendriplex in D_2O is dominated by the dendrimer, as its neutron SLD contrast is about 1.8 times that of DNA.[27]

The dominance of the constituents on scattering intensity was demonstrated by the neutron contrast matching experiment. Figure 1 shows the SANS profiles of the dendriplex with dp/0.7 dendrimer ($(N/P)_n$ = 6) suspended in D_2O and 35/65 (v/v) D_2O/H_2O mixture. The later mixed solvent was able to match the neutron SLD of PAMAM dendrimer, such that the SANS intensity was contributed by DNA. It can be seen that the SANS profile of the dendriplex in D_2O exhibited a small peak at 1.41 nm^{-1} associated with the dendrimer-dendrimer correlation. This small peak vanished in the SANS profile collected with 35/65 D_2O/H_2O mixture, where a stronger peak contributed by the DNA component was identified at 2.40 nm^{-1}. The corresponding SAXS profile of the dendriplex is also displayed in the figure for comparison. Both the small and strong peaks were observable in the SAXS curve, with the DNA peak (at ca. 2.3 nm^{-1}) being stronger than the dendrimer peak (at ca. 1.4 nm^{-1}). It is noted that the peaks in the SANS profiles were located at slightly higher q than the corresponding ones in the SAXS curve. This may be due to the fact that the dendrimer component may still make a minor contribution to the X-ray scattering intensity and the addition of this component to the DNA contribution could slightly move the peak positions. However, the results in Figure 1 verified that DNA gave rise to much stronger X-ray scattering than dendrimer in the dendriplex; therefore, the SAXS profiles were mainly used to reveal the structure of DNA in the dendriplex, while the SANS curves of the dendriplexes in D_2O were employed to resolve the organization of dendrimer, as the neutron SLD contrast of DNA in D_2O is much smaller than that of dendrimer. These two scattering techniques are indeed complementary to each other for the structural characterization of the dendriplex.

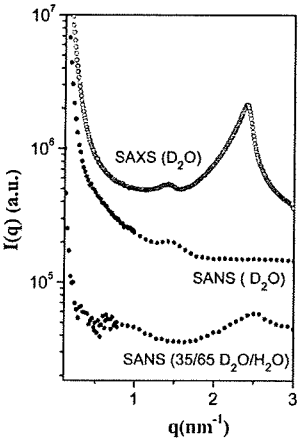

Figure 1. SANS and SAXS profiles of the complex of DNA with PAMAM G4 dendrimer with dp =0.7 to demonstrate the dominance of the constituents on scattering intensity. The nominal N/P ratio was 6.0. The SANS profiles were collected for the dendriplexes suspended in D_2O and 35/65 (v/v) D_2O/H_2O mixture. The later mixed solvent was able to match the neutron SLD of PAMAM dendrimer, such that the SANS intensity was contributed by DNA.

1. The Three Distinct Types of Structure. Before demonstrating the effects of the system parameters on the dendriplex structure, we would like to present the three types of structure formed by G4 dendriplex and the features of their scattering patterns. Although these structures had been identified previously in a brief report,[35] the analyses of their small-angle scattering patterns have been refined here to provide more detailed description of the structure features. Moreover, the actual N/P ratios associated with different types of structure will be calculated from the combination of SAXS and SANS results to facilitate the identification of the key thermodynamic driving forces underlying the structural formation.

Figure 2 displays the representative SAXS and SANS profiles (collected in D_2O) of the dendriplexes as a function of the dp value of the dendrimer. The nominal N/P ratio was fixed at 6. Four distinct types of SAXS profiles were observed (see Figure 2a), while the SANS profiles of all dendriplexes were similar, showing only a relatively broad peak at 1.4−1.6 nm^{-1} (see Figure 2b). Consequently, the organization of dendrimer in the complexes was quite similar, but the structure of DNA strongly depended on dendrimer charge density.

Structure 1. Square Columnar Phase. The complex with the dendrimer of low charge density (dp = 0.1) exhibited three diffraction peaks with the position ratio of $1:2^{1/2}:4^{1/2}$ in the SAXS profile, indicating that the system formed a square columnar phase (denoted by "SQ"), where the locally straightened DNA chains packed in a 2D square lattice.[29,31,33,35] The interhelical distance of DNA (d_{DNA}) in the square lattice was 4.1 nm as calculated from the primary peak position (q_m) via $d_{DNA} = 2\pi/q_m$. The formation of the 2D square lattice has also been confirmed by the TEM reported in our previous study.[26]

The corresponding SANS profile showed only one peak (marked by the arrow in Figure 2b) at ca. 1.5 nm^{-1}. This peak was attributed to the nearest-neighbor distance between the dendrimer molecules located in the interstitial tunnels in the

dx.doi.org/10.1021/ma500546h | Macromolecules 2014, 47, 3117−3127

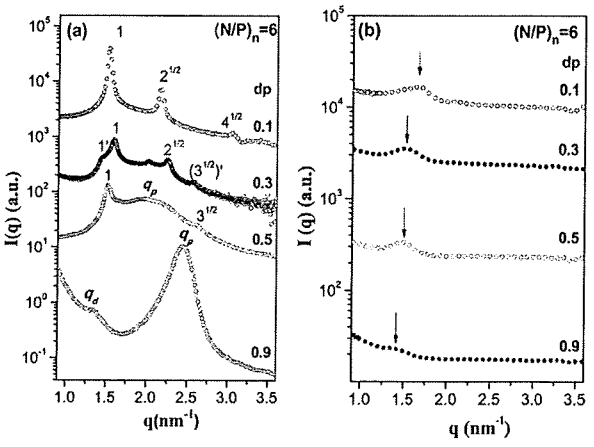

Figure 2. (a) SAXS and (b) SANS profiles (collected in D_2O) of the dendriplexes as a function of the dp value of the dendrimer. The nominal N/P ratio was fixed at 6. Four distinct types of SAXS profiles were observed, while the SANS profiles of all dendriplexes were similar, showing only a relatively broad peak (pinpointed by the arrow) at 1.4–1.6 nm^{-1}.

square lattice. This postulate was verified by calculating the scattering profiles of the SQ phase by the Debye equation.[40] Here we constructed a square lattice of DNA (represented by rigid cylinder with the diameter of 2 nm) composed of four unit cells (Figure 3a). The dendrimer molecules (represented by spheres with the diameter of 4 nm) were placed in the tunnel regions between DNA in such a way that there existed a characteristic interparticle distance (d_{den}) along the DNA length axis (or (01) direction of the lattice), as shown in Figure 3a. The structure model was then divided into numerous volume elements (each has the volume of 0.5 × 0.5 × 0.5 nm^3), and the partial structure factors associated with the DNA–DNA correlation $S_{DD}(q)$, DNA-dendrimer correlation $S_{Dd}(q)$, and dendrimer-dendrimer correlation $S_{dd}(q)$ were calculated by the Debye equation, viz.[28]

$$S_{dd}(q) = \sum_{i\in G4}\sum_{j\in G4}\frac{\sin(q|\mathbf{r}_i - \mathbf{r}_j|)}{q|\mathbf{r}_i - \mathbf{r}_j|} \quad (1)$$

$$S_{DD}(q) = \sum_{i\in DNA}\sum_{j\in DNA}\frac{\sin(q|\mathbf{r}_i - \mathbf{r}_j|)}{q|\mathbf{r}_i - \mathbf{r}_j|} \quad (2)$$

$$S_{Dd}(q) = \sum_{i\in DNA}\sum_{j\in G4}\frac{\sin(q|\mathbf{r}_i - \mathbf{r}_j|)}{q|\mathbf{r}_i - \mathbf{r}_j|} \quad (3)$$

where $|\mathbf{r}_i - \mathbf{r}_j|$ is the distance between i and j volume element in the model.[41] The SAXS and SANS intensities were then obtained from the three partial structure factors by the following equation[27,35]

$$I(q) = \Delta\rho_{DNA}{}^2 S_{DD}(q) + 2\Delta\rho_{DNA}\Delta\rho_{den}S_{Dd}(q) + \Delta\rho_{den}{}^2 S_{dd}(q) \quad (4)$$

where $\Delta\rho_{DNA}$ and $\Delta\rho_{den}$ are the SLD contrast of DNA and dendrimer, respectively. The calculated scattering profiles of the SQ phase are displayed in Figure 3b. It can be seen that the calculated SAXS profile exhibited a series of diffraction peaks characteristic to the square packing of DNA. The calculated SANS profile showed a relatively broad peak (q_{den}), consistent with the experimental observation. The position of this peak is determined by the interparticle distance between the dendrimer molecules along the tunnel, i.e., $d_{den} = 2\pi/q_{den}$ (see Figure 3b); therefore, d_{den} in the dp/0.1 dendriplex was 4.3 nm according to the SANS peak position. Knowing the value of d_{den}, the actual N/P ratio of the dendriplex, $(N/P)_a$, can be calculated by

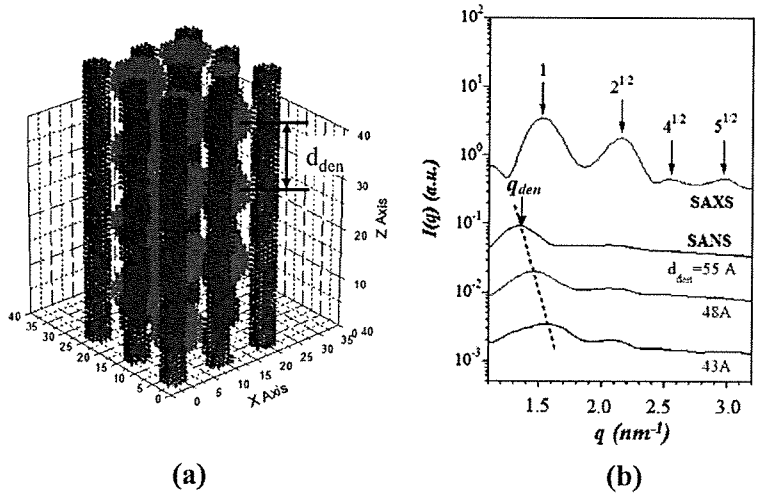

Figure 3. (a) Structure model used to calculate the scattering profiles of the SQ phase. The model composed of four unit cells of the square-packed DNA (represented by rigid cylinders with the diameter of 2 nm). The dendrimer molecules (represented by spheres with the diameter of 4 nm) were placed in the tunnel regions between DNA in such a way that there existed a characteristic interparticle distance (d_{den}) along the DNA length axis. (b) SAXS and SANS profiles calculated using the model in part a. Different values of d_{den} were assumed in the calculation of SANS profile to demonstrate that the position of the scattering peak (q_{den}) was determined by d_{den} via $d_{den} = 2\pi/q_{den}$.

dx.doi.org/10.1021/ma500546h | Macromolecules 2014, 47, 3117–3127

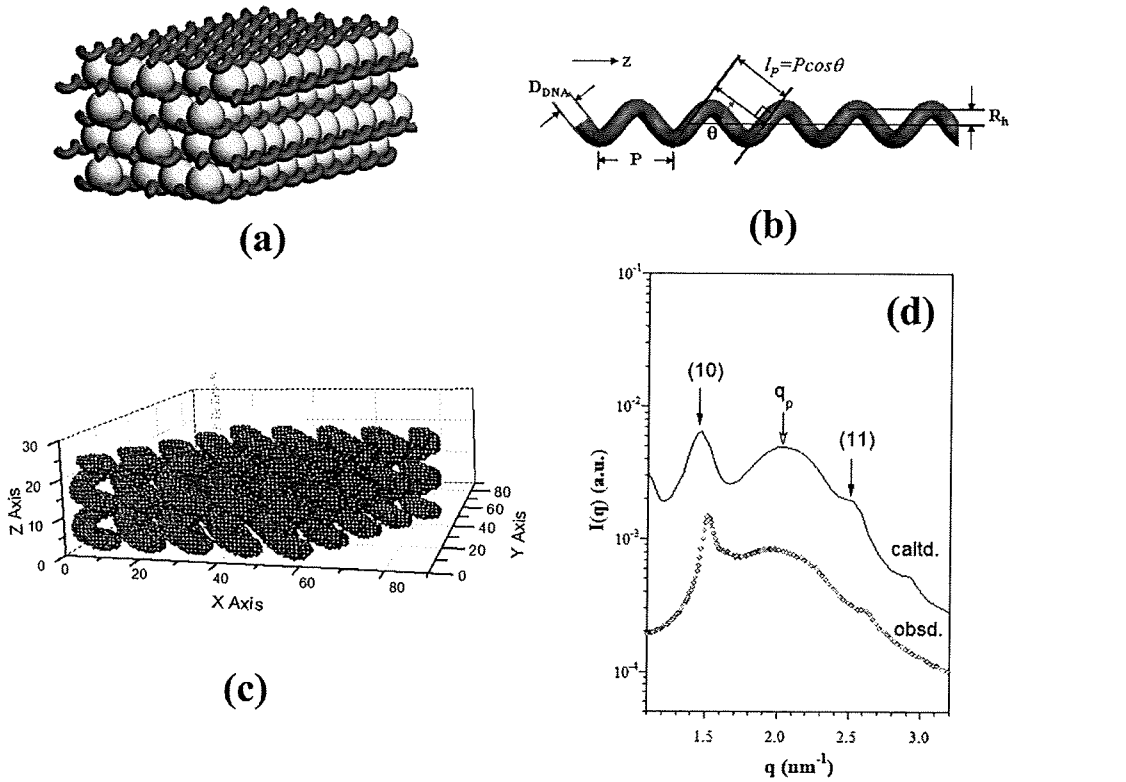

Figure 4. (a) Schematic illustration of HEX_h structure. (b) Schematic illustration of a DNA superhelix and the definitions of the geometric parameters used for calculating SAXS profile. P and θ represent the pitch length and pitch angle, respectively. R_h is the radius of the superhelix defined as the radial distance between the centerline and central trace of the helix. (c) Structure model used to calculate the SAXS profile of the HEX_h structure. The model composed of eight unit cells with the following parameter values: D_{10} = 4.3 nm, DNA superhelix length =11 nm, P = 4 nm and R_h = 2.3 nm. The helical traces of all superhelics in the lattice were assumed to be in phase. (d) Comparison between the observed SAXS profile of dp/0.5 dendriplex and the calculated curve of HEX_h structure. The agreement is fairly good.

$$\left(\frac{N}{P}\right)_a = \frac{\text{number of amine groups per dendrimer molecule}}{d_{den}\ (\text{linear charge density of DNA})}$$

$$= \frac{126}{4.3\ \text{nm} \times \left(\frac{\text{20 phosphate groups per pitch length of DNA duplex}}{\text{3.4 nm in pitch length}}\right)}$$

$$= 5.0$$

Structure 2. Hexagonally Packed DNA Superhelices. The second type of SAXS pattern was observed for the dendriplex with intermediate dp value (e.g., dp = 0.5), where the scattering profile exhibited two relatively sharp peaks with the position ratio of $1:3^{1/2}$ along with a broad peak (marked by "q_p") between them. The observed SAXS profile was attributed to a new type of mesophase called "hexagonally-packed DNA superhelices (denoted as "HEX_h"),[35] as schematically illustrated in Figure 4a. Here we also calculated the SAXS profile associated with the model structure using the Debye equation to demonstrate that HEX_h can yield the observed SAXS pattern. Since SAXS intensity is dominated by DNA, only DNA superhelices were placed in the lattice for calculating the SAXS profile. The DNA superhelix was approximated by a uniform helical cylinder with a given pitch length P and pitch angle θ (see Figure 4b).[22] The radius of the superhelix (R_h) given by $R_h = P/(2\pi \tan \theta)$ is defined as the radial distance between the centerline and central trace of the helix (R_h = 0 for completely straight DNA). The helical trace of the cylinder was then calculated from the following equations[42]

$$x(z) = R_h \sin\left(\frac{2\pi z}{P} + \phi\right); \quad y(z) = R_h \cos\left(\frac{2\pi z}{P} + \phi\right)$$

where ϕ is the phase angle that defines the sense of the superhelix. Figure 4c shows the 3D presentation of HEX_h structure composed of eight unit cells with the following parameter values: D_{10} = 4.3 nm, DNA superhelix length = 11 nm, P = 4 nm, and R_h = 2.3 nm. The helical traces of all superhelics in the lattice were assumed to be in phase. The calculated SAXS profile was compared with the experimentally observed one in Figure 4d. It can be seen that the agreement was fairly good. The q_p peak situating between the (10) peak and the (11) peak of the hexagonal lattice was associated with the pitch of the superhelices. The intensity of this peak relative to (10) peak depended on the length and R_h of the DNA superhelix assumed for the calculation, where the smaller the length and R_h, the weaker the q_p peak. The intensity of the q_p peak also decreased if we allowed the phase of the helical traces of the superhelices to fluctuate in the lattice.

The SANS profile associated with the HEX_h phase also exhibited a broad peak at ca. 1.5 nm^{-1} (see Figure 2b), which was again attributable to the interparticle distance (d_{den} = 4.18 nm) between the dendrimer molecules along the length direction of the superhelices. Because the pitch length was about the same as d_{den}, we assumed that a dendrimer molecule was accommodated within a groove (with the projected length of P on the helix axis)

dx.doi.org/10.1021/ma500546h | Macromolecules 2014, 47, 3117–3127

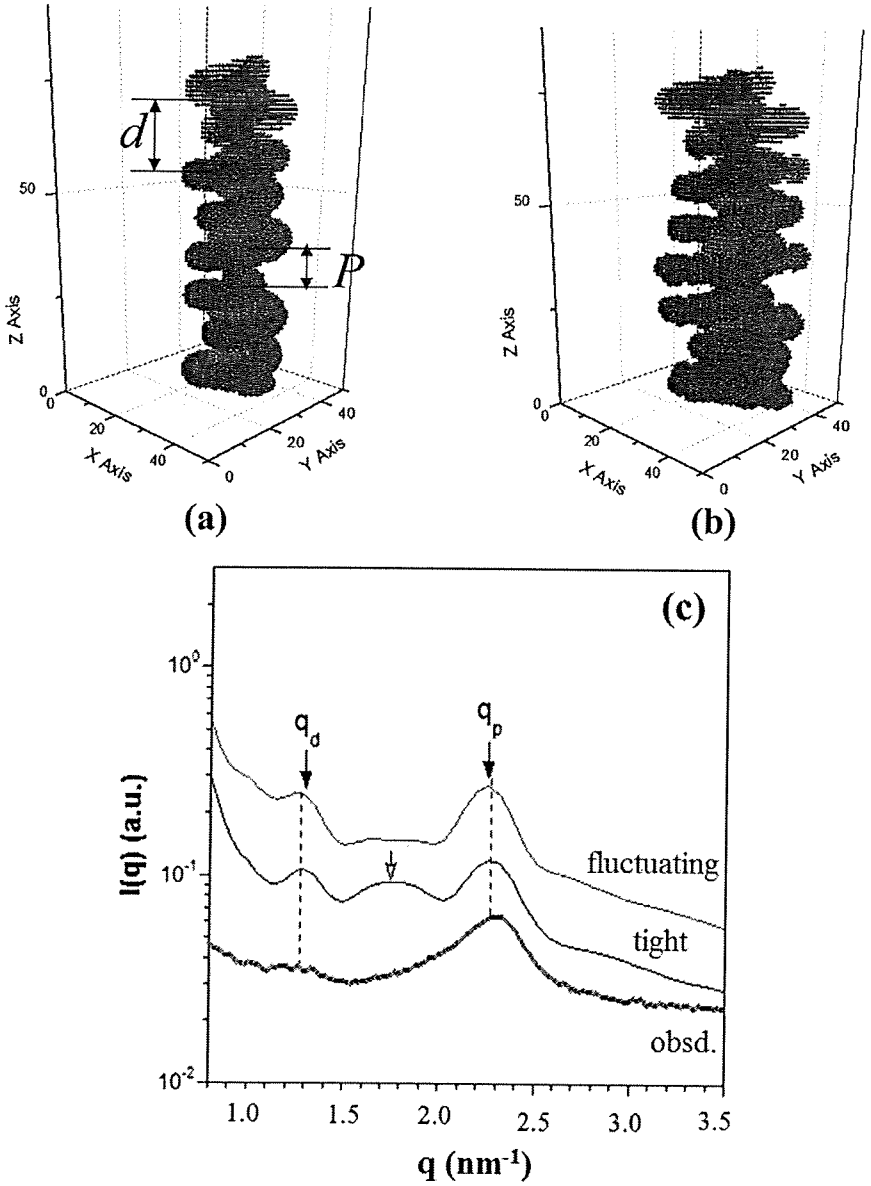

Figure 5. Model of the beads-on-string structure used to calculate the SAXS profile and the calculated SAXS curves. (a) Stiff chromatin-like fiber with DNA wrapping around the dendrimer tightly. (b) Stiff chromatin-like fiber with fluctuating DNA superhelix under a give pitch length. (c) Comparison between the observed and calculated SAXS profiles.

of the superhelix, then the actual N/P ratio associated with the HEX_h structure was given by

$$(N/P)_a = [126 \text{ amine groups in a dendrimer molecule}] / (\text{arc length of DNA over the pitch length}) (\text{linear charge density of DNA}) \approx 1.5$$

Structure 3. Beads-on-String Structure. As can be seen in Figure 2, the third type of scattering pattern observed at high dendrimer dp (e.g., dp = 0.9) shows a small peak at 1.4 nm^{-1} (marked by "q_d") and a strong peak (marked by "q_p") at 2.4 nm^{-1}. This scattering pattern has been attributed to the beads-on-string structure (denoted by "BOS") formed by DNA wrapping around the dendrimer[35] We called the basic building block with DNA wrapping around a dendrimer molecule "a nucleosome-like particle".[27,35] Since the length of DNA studied here was much larger than the periphery of the dendrimer, each DNA chain was able to wrap around a number of dendrimer molecules to yield the "chromatin-like fiber" composed of interconnected nucleosome-like particles, as schematically illustrated in Figure 5a. The chromatin-like structure is characterized by two parameters, namely, the nearest-neighbor distance (d) between the nucleosome-like particles in the fiber and the pitch length (P) of the DNA superhelix wrapping around the dendrimer (Figure 5a).[27,28,35]

dx.doi.org/10.1021/ma500546h | *Macromolecules* 2014, 47, 3117–3127

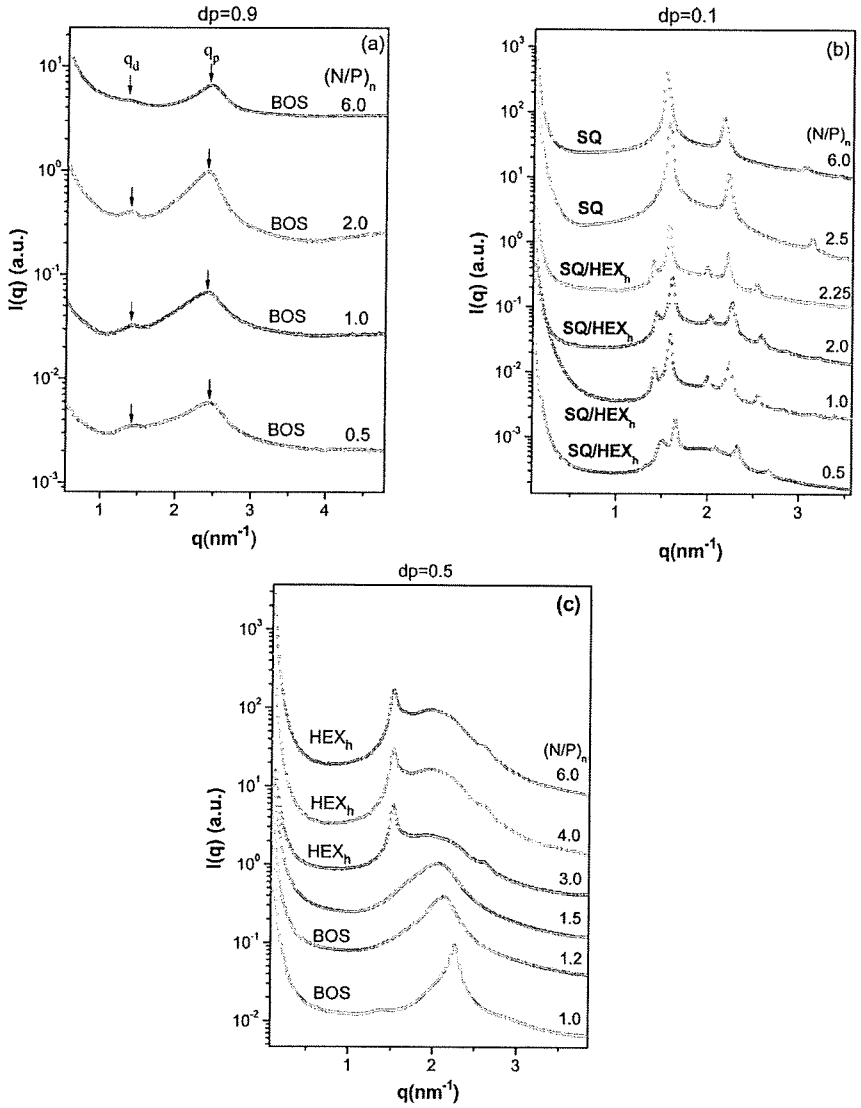

Figure 6. SAXS profiles of the dendriplexes as a function of $(N/P)_n$ under fixed dendrimer dp values of (a) 0.9, (b) 0.1, and (c) 0.5. The dp/0.9 dendriplex always formed BOS structure irrespective of $(N/P)_n$. The situation became different at sufficiently low dp (dp $\leq$0.5), where the nominal N/P ratio was found to influence the structure obviously.

The scattering profile associated with BOS structure was also calculated and compared with the experimental result to verify the formation of such a structure at high dendrimer charge density. We first assumed that DNA wrapped around the dendrimer tightly with the pitch length of 2.9 nm, as shown in Figure 5a; the SAXS profile of a rigid chromatin-like fiber composed of five nucleosome-like particles with d = 4.5 nm was then calculated using the Debye equation and the calculated result is shown in Figure 5c. The assumed structure generated a small q_d peak at 1.4 nm^{-1} prescribed by the value of d ($=2\pi/q_d$) and a strong q_p peak given by the pitch length ($P \sim 2\pi/q_p$) in the SAXS profile, which was consistent with the experimental result. It is noted that the pitch peak appeared clearly in the calculated SAXS profile only when the coherent correlation between the helical segments spaced by the pitch length was strong. This occurred when DNA wrapped *uninterruptedly* around more than three G4 dendrimer molecules along the chromatin-like fiber axis (i.e., the helical trace of DNA continued over sufficiently long distance). If the wrapping was interrupted, for instance, by a linker DNA, the corresponding SAXS pattern was just characterized by the form factor maxima of the DNA superhelix in a single nucleosome-like particle.

As can be seen in Figure 5c, the tight wrapping yields a clear peak (marked by the open arrow) situating between q_d and q_p peak, which was not observed clearly in the experimental SAXS profile. This peak is the first-order form factor maximum of the DNA superhelix as its position depends on the average R_h of the superhelix. In the previous report, we assumed that the DNA superhelix penetrated by a depth into the dendrimer while wrapping around it; the reduction of R_h due to such a penetration shifted the superhelix form factor maximum to higher q and its overlap with the pitch peak made it indistinguishable experimentally. Nevertheless, the bending energy of DNA wrapping tightly around the relatively small G4 dendrimer

dx.doi.org/10.1021/ma500546h | *Macromolecules* 2014, 47, 3117−3127

(diameter ~4 nm) should be quite large, the radial penetration of DNA further increased such an energetic penalty and may thus be unfavorable.

Another more plausible model that may account for the invisible superhelix form factor peak is the fluctuation of the R_h of the DNA superhelix. In this case, DNA wrapped around the dendrimers loosely, with its R_h fluctuating about a mean value, as shown in Figure 5b. The fluctuation led to a broad distribution of R_h, that smeared out the form factor maximum of the superhliex. In the program for calculating the scattering profile of the fluctuating chromatin-like fiber, we set a maximum value of 2 nm for the fluctuation of R_h, ΔR_{max}, and the R_h value of each turn in the wrapping under a given pitch length was assigned randomly by the computer as $R_h = R_{h0} \pm \Delta R$ (with $\Delta R \leq \Delta R_{max}$), where R_{h0} is the radius of the tight-wrapping superhelix. Figure 5b displays a representative image of the fluctuating chromatin-like fiber generated by the computer. Since each image only represented a snapshot of the constantly fluctuating structure, the SAXS profile of the chromatin-like fiber was obtained by averaging the scattering curves of 10 snapshots. The SAXS curve thus obtained is shown in Figure 5c. It can be seen that the calculated SAXS curve closely agreed with the experimentally observed profile, as the form factor maximum of the superhelix was hardly observable; therefore, we postulate that DNA wrapped around the dendrimer molecules at high charge density with fluctuating superhelix radius. The fluctuation of DNA may be caused by the thermal fluctuations of the monomer units constituting the dendrimer.

It is difficult to calculate the accurate value of the actual N/P ratio of the fluctuating beads-on-string structure. Here we assumed that the average radius of the fluctuating DNA superhelix was approximately the same as that of the superheix with tight wrapping, then $(N/P)_a$ is given by

$$(\mathrm{N/P})_a = [126 \text{ amine groups in a dendrimer molecule}] / (\text{arc length of DNA wrapping tightly around a dendrimer})(\text{linear charge density of DNA}) \approx 0.9$$

Coexistence of SQ and HEX_h Phases. In addition to the three characteristic scattering patterns, another SAXS profile composed of a large number of peaks was identified under certain condition (e.g., for dp/0.3 dendriplex in Figure 2). This scattering profile appeared like the supposition of the peaks from the SQ and HEX_h phase; therefore, it was considered as an indicative of the coexistence of the two types of structure in the dendriplex.

No other scattering pattern was observed for the dendriplexes with any combination of dp and $(N/P)_n$ besides the four types of SAXS profiles displayed in Figure 2. The actual N/P ratio of the dendriplex decreased from SQ to HEX_h to BOS structure. This is easily understandable, because there are more phosphate groups interacting with a given dendrimer macrocation when the tertiary structure of DNA adopts a higher curvature.

2. The Effect of Dendrimer Charge Density under Fixed Nominal N/P Ratio. Figure 2 has already revealed that under a given nominal N/P ratio of 6.0, increasing the charge density of G4 dendrimer induced the transformation of the dendriplex structure from SQ phase to SQ/HEX_h coexistence to HEX_h phase and eventually to BOS structure. This sequence of structure transformation with respect to the increase of dendirmer dp was also observed for other nominal (N/P) ratios (see Figure S1 of the Supporting Information), although in some cases not all these structures were accessible. The observed phase transition sequence indicates that DNA tended to enhance the charge matching with dendrimer when the charge density of the dendrimer was increased.

It is noted that the scattering profiles associated with a given type of structure were virtually the same (except for slight difference in peak position) irrespective of dendrimer dp and $(N/P)_n$. For instance, the scattering profiles associated with the SQ phase formed by dp/0.1 and dp/0.2 dendrplex with $(N/P)_a$ = 6 were almost identical (see Figure S2 of the Supporting Information). This implies that a given type of structure was characterized by a well-defined composition or $(N/P)_a$, and the structure with such a composition existed over a certain range of dp.

3. The Effect of Nominal N/P Ratio under a Given Dendrimer dp. In the case of high dendrimer dp (e.g., dp $\geq$ 0.6), the dendriplex always formed BOS structure irrespective of $(N/P)_n$, as demonstrated in Figure 6a. The situation became different at sufficiently low dp (dp $\leq$ 0.5), where the nominal N/P ratio was found to influence the structure obviously. Figure 6b displays the SAXS profiles of dp/0.1 complex as a function of $(N/P)_n$. It can be seen that at $(N/P)_n \geq 2.5$ the complex exhibited SQ phase. Reducing the nominal N/P ratio to below 2.5 induced the formation of HEX_h structure coexisting with the SQ phase. The structural transformation induced by changing $(N/P)_n$ was even more obvious for dp/0.5 complex, as demonstrated in Figure 6c. Here the dendriplex displayed HEX_h structure at $(N/P)_n \geq 3.0$, but the structure transformed to BOS when $(N/P)_n$ was lowered to 1.2. Figure 6 clearly revealed that reducing the nominal N/P ratio exerted the same effect as increasing dendrimer dp value. That is, the system tended to form the structure with better charge matching at the lower nominal N/P ratio.

4. Morphological Diagram. Through probing the structures of the complexes over a broad range of combination of dp and nominal N/P ratio, we have constructed the morphological diagram for the dendriplex prepared with the DNA concentration of 2 mg/mL, as shown in Figure 7. It can be seen that, under a given $(N/P)_n$, increasing dendirmer charge density tended to induce the formation of the structure offering better charge matching. The morphological diagram shows that

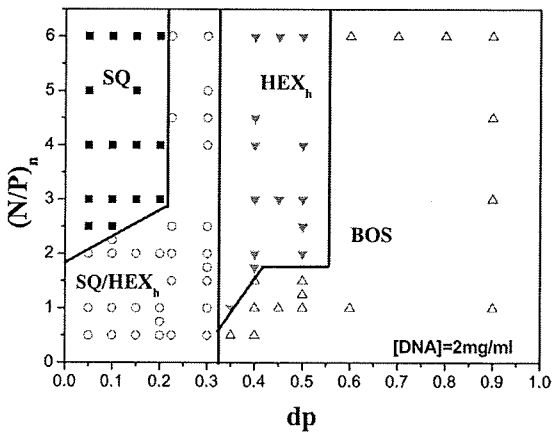

Figure 7. Morphological diagram of the dendriplex prepared with the DNA concentration of 2 mg/mL.

dx.doi.org/10.1021/ma500546h | Macromolecules 2014, 47, 3117–3127

the structure was insensitive to the nominal N/P ratio at intermediate dp (= 0.22−0.3) and high dp (dp ≥0.6), but structural transformation induced by the change of $(N/P)_n$ became accessible at dp < 0.22 and 0.3 < dp < 0.6, where decreasing $(N/P)_n$ favored the structure with higher degree of charge matching. In this case, the BOS structure was accessible at low $(N/P)_n$ even when only 30% amine groups on the dendrimer were charged.

DISCUSSION

Our SAXS results have revealed that dendrimer charge density and nominal (N/P) ratio are two key parameters for tuning the structure of G4 dendriplex. The morphological diagram obtained is indeed quite complicated and quantitative prediction of the structural transitions in the diagram is beyond the scope of the present work. Here we attempt to seek a qualitative understanding on the tendency of structural transformation by considering the interplay between DNA bending energy and the free energy of charge matching mediated by the two parameters. The free energy of charge matching composes of two terms, namely, the free energy of electrostatic attraction between DNA and dendrimer and the free energy arising from the entropic gain from the release of Na^+ and Cl^- counterions originally condensed on DNA and dendrimer, respectively, when the positive charges of the ammonium groups in dendrimer are matched by the negative charges of the phosphate groups in DNA. Within the context of Manning condensation,[43−45] a large fraction of counterions should have already condensed on DNA and dendrimer by electrostatic attraction before complexation; therefore, the free energy reduction by the electrostatic attraction between ammonium and phosphate groups upon complexation may not be large enough to compensate or outweigh DNA bending energy to form the structure with large DNA curvature (e.g., HEX_h and BOS structure) for achieving high degree of charge matching. The factor that drives the system to achieve high degree of ammonium-phosphate charge matching is hence the entropic gain from the release of the condensed counterions into the bulk solution. This factor wrestles against the DNA bending energy, and the type of structure formed is governed by such an interplay.

The increase of degree of charge matching upon increasing dendrimer dp value can hence be attributed to the tendency of the system to release as many counterions condensed on the dendrimer as possible under the constraint of DNA bending energy. A simple understanding of this phenomenon may be depicted as follows. The positive/negative charge ratio (n_+/n_-) associated with a specific type of structure is simply given by $(N/P)_a \times (dp)$. According to our calculation, the actual N/P ratio of SQ phase was about 5.0; therefore, all the counterions on the dendrimer may be released without DNA bending as long as the dp value was lower than 0.2. However, when the dp value exceeded 0.2, DNA had to bend to enhance the charge matching for releasing all counterions on the dendrimer. The formation of HEX_h structure (which prescribes the positive/negative charge ratio of 1.5 × dp) would allow all counterions to be released until the charge density reached ca. 0.67. For dp higher than 0.67 BOS structure formed to further increase the number of released counterions. This argument qualitatively explains why the curvature of DNA in the dendriplex increased with increasing dendrimer charge density.

The above argument only considered the effectiveness of counterion release, while the bending energy cost was not taken into account. At sufficiently high dendrimer charge density (dp > 0.5), because there were a large number of counterions condensed on dendrimer originally, the tendency to release all these counterions may outweigh DNA bending energy, such that the dendriplex always formed BOS structure irrespective of $(N/P)_n$.

However, consideration of the interplay between the tendency to release all condensed counterions and DNA bending energy still failed to explain why the structure would depend on the nominal N/P ratio, which was observed over some range of dp values. For instance, at $(N/P)_n$ < 2, SQ phase became inaccessible even when the dp value was as low as 0.05 (see Figure 7). In this case, the formation of SQ phase was able to release all counterions without the cost of DNA bending energy, but why did DNA choose to bend under this condition?

Indeed, the tendency of structural transition with respect to the change of $(N/P)_n$ implies that the system attempted to form the structure with smaller actual N/P ratio when the nominal N/P ratio was lower, and vice versa. This further implies that there existed a driving force which tended to reduce the concentration of free DNA or free dendrimer in the bulk solution. For instance, if the nominal N/P ratio is 0.9, there will be no free polyelectrolytes remained in the solution if the complex forms BOS structure, since the dendriplex precipitates out from the solution; however, a great amount of free DNA will remain in the solution if the dendriplex forms SQ structure.

Now the question is why the system tended to reduce the free polyelectrolyte concentration in the bulk solution ? We propose that this is again associated with the entropy of the counterions released to the bulk solution. Since the free polyelectrolytes occupy a fraction of the space over which the counterions can move around in the solution, incorporating them into the complex can increase the translational entropy of the counterions. To the first order of approximation, we assume that the counterions are noninteracting mass points with negligible volume. Their translational entropy in the bulk solution is then given by

$$S_{trans} \sim N_i k_B \ln(V_{solvent} - V_{PE,f}) \quad (5)$$

where N_i is the number of counterions released, $V_{solvent}$ is the volume of solvent, and $V_{PE,f}$ is the volume occupied by the free polyelectrolytes. $(V_{solvent} - V_{PE,f})$ is simply the volume available for the counterions to move around in the solution. At high dendrimer dp where there were a lot of condensed Cl^- counterions, the dendriplex formed the structure which provided high degree of charge matching (e,g, BOS structure) to release the maximum number of counterions, because increasing N_i increased the counterion entropy. In this case, the term N_i dominated the counterion entropy expressed by eq 5. At lower dendrimer dp, N_i became small even if all Cl^- counterions were released, the volume available for counterion movement may govern the entropy. In this case, the system tended to reduce the concentration of free DNA or dendrimer in the bulk solution to increase the translational entropy of the counterions. Therefore, the structure with higher DNA curvature became more favored at the lower nominal N/P ratio, and vice versa.

The important role of the counterion entropy in the structural formation of the dendriplex was verified by preparing the dendriplex with a given combination of dp and nominal N/P ratio using different DNA concentrations. Figure 8 displays the SAXS profiles of the dendriplex with dp = 0.1 and $(N/P)_n = 6$. The DNA concentrations used for preparing the dendriplex are marked in the figure. Since $(N/P)_n$ was fixed, the concentration of dendrimer was lower when the DNA concentration was lower.

dx.doi.org/10.1021/ma500546h | Macromolecules 2014, 47, 3117−3127

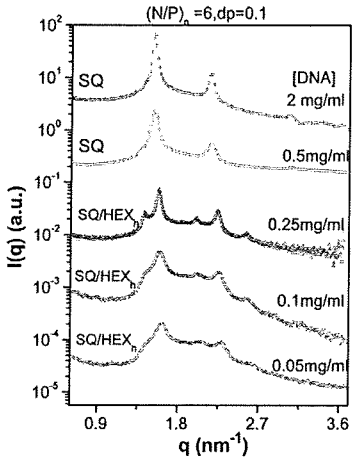

Figure 8. SAXS profiles of the dendriplex with dp = 0.1 and $(N/P)_n = 6$ prepared with different initial concentrations of DNA. The DNA concentrations are marked in the figure.

The dendriplexes prepared with DNA concentration of 2 and 0.5 mg/mL formed SQ structure. Upon decreasing DNA concentration to 0.25 mg/mL and below, the SAXS profiles revealed the coexistence of SQ phase and HEX_h structure. The results indicate that at lower polyelectrolyte concentration for complex preparation, the system tended to release more counterions by introducing DNA curvature, because the concentration of the fee polyelectrolytes remained in the bulk solution was lower for lower initial concentration. In this case, the counterions, once released, can enjoy a greater space for gaining higher translational entropy. As a result, the structure with greater DNA curvature tended to form at lower initial polyelectrolyte concentration. The present study demonstrates the crucial role of counterion entropy in the structure formation of dendriplex and such an entropic contribution is related to three system parameters, namely, dendrimer charge density, nominal N/P ratio, and polyelectrolyte concentration adopted for complex preparation.

CONCLUSIONS

Complexes of DNA with PAMAM G4 dendrimer were found to display three distinct types of structure governed by the dendrimer dp value and nominal N/P ratio. The structure tended to transform from SQ to coexistent state to HEX_h to BOS with increasing dendrimer dp under a fixed $(N/P)_n$. Decreasing $(N/P)_n$ exerted the same effect as increasing dendrimer dp, especially for the dendriplexes with relatively low dednrimer dp. This phenomenon was attributed to the additional driving force which tended to minimize the concentration of free DNA or dendrimer in the bulk solution for increasing the translational entropy of the counterions released upon complexation. This entropy-driven effect was further verified by examining the influence of the initial concentrations of DNA and dendrimer used for complex preparation, where the use of lower concentration favored the formation of the structure with larger DNA curvature. The present study revealed the central role of counterion entropy in tuning the self-assembled structure of DNA–dendrimer complexes, where dendrimer charge density nominal N/P ratio and initial concentration of the polyelectrolytes are the key parameters controlling the cotribution of this entropic factor relative to the bending energy of DNA.

ASSOCIATED CONTENT

Supporting Information

Determination of the average degree of protonation of PAMAM G4 dendrimer, SAXS and SANS profiles of DNA-PAMAM G4 dendriplexes as a function dendrimer dp values under the fixed $(N/P)_n$ ratios, and SAXS and SANS profiles of dp/0.1 and dp/0.2 dendriplexes with $(N/P)_n = 6$ to demonstrate that the scattering profiles associated with a given type of structure were virtually the same. This material is available free of charge via the Internet at http://pubs.acs.org.

AUTHOR INFORMATION

Corresponding Author

*(H.-L.C.) E-mail: hlchen@che.nthu.edu.tw.

Notes

The authors declare no competing financial interest.

ACKNOWLEDGMENTS

We acknowledge the financial support of the National Science Council (NSC), Taiwan under Grant No. NSC 100-2923-E-007-003. We also thank the Neutron User Program of the NSC for providing the financial support for carrying out the SANS experiments. The support for the SANS beamtime at EQ-SANS by SNS, Oak Ridge National Laboratory, Oak Ridge, TN, is also gratefully acknowledged.

REFERENCES

(1) Chiou, H. C.; Tangco, M. V.; Kormis, K.; Levine, S. M.; Robertson, D.; Kormis, K.; Wu, C. H.; Wu, G. Y. *Nucleic Acids Res.* **1994**, *22* (24), 5439–5446.

(2) Hudde, T.; Rayner, S. A.; Comer, R. M.; Weber, M.; Isaacs, J. D.; Waldmann, H.; Larkin, D. P. F.; George, A. J. T. *Gene Ther.* **1999**, *6*, 939–943.

(3) Eichman, J. D.; Bielinska, A. U.; Kukowska-Latallo, J. F.; Baker, J. R., Jr *Pharm. Sci. Technol. Today* **2000**, *3*, 232–245.

(4) Manunta, M.; Tan, P. H.; Sagoo, P.; Kashefi, K.; George, A. J. T. *Nucleic Acids Res.* **2004**, *32*, 2730–2739.

(5) Seib, F. P.; Jones, A. T.; Duncan, R. *J. Controlled Release* **2007**, *117*, 291–300.

(6) Perumal, O. P.; Inapagolla, R.; Kannan, S.; Kannan, R. M. *Biomaterials* **2008**, *29*, 3469–3476.

(7) Deng, R.; Yue, Y.; Jin, F.; Chen, Y.; Kung, H.-F.; Lin, M. C. M.; Wu, C. *J. Controlled Release* **2009**, *140*, 40–46.

(8) Yue, Y.; Wu, C. *Biomat. Sci.* **2013**, *1*, 152–170.

(9) Dai, Z. J.; Wu, C. *Macromolecules* **2012**, *45*, 4346–4353.

(10) Haxton, T. K.; Whitelam, S. *Soft Matter* **2012**, *8*, 3558–3562.

(11) Kostiainen, M. A.; Hiekkataipale, P.; Laiho, A.; Lemieux, V.; Seitsonen, J.; Ruokolainen, J.; Ceci, P. *Nat. Nano.* **2013**, *8*, 52–56.

(12) Koltover, I.; Salditt, T.; Safinya, C. R. *Biophys. J.* **1999**, *77*, 915–924.

(13) Tomalia, D. A.; Baker, H.; Dewald, J.; Hall, M.; Kallos, G.; Martin, S.; Roeck, J.; Ryder, J.; Smith, P. *Polym. J.* **1985**, *17*, 117–132.

(14) Esfand, R.; Tomalia, D. A. *Drug Discovery Today* **2001**, *6*, 427–436.

(15) Newkome, G. R. *Advances in Dendritic Macromolecules*; JAI Press: Greenwich, CT, 1993.

(16) Naylor, A. M.; Goddard, W. A.; Kiefer, G. E.; Tomalia, D. A. *J. Am. Chem. Soc.* **1989**, *111*, 2339–2341.

(17) Tomalia, D. A.; Uppuluri, S.; Swanson, D. R.; Li, J. *Pure Appl. Chem.* **2000**, *72*, 2343–2358.

(18) Tomalia, D. A. *Chim. Oggi.* **2005**, *23*, 41–45.

(19) Porcar, L.; Liu, Y.; Verduzco, R.; Hong, K. L.; Butler, P. D.; Magid, L. J.; Smith, G. S.; Chen, W. R. *J. Phys. Chem. .B* **2008**, *112*, 14772–14778.

(20) Li, T. F.; Hong, K.; Porcar, L.; Verduzco, R.; Butler, P. D.; Smith, G. S.; Liu, Y.; Chen, W. R. *Macromolecules* **2008**, *41*, 8916–8920.

(21) Liu, Y.; Chen, C.-Y.; Chen, H.-L.; Hong, K.; Shew, C.-Y.; Li, X.; Liu, L.; Melnichenko, Y. B.; Smith, G. S.; Herwig, K. W.; Porcar, L.; Chen, W.-R. *J. Phys. Chem. Lett.* **2010**, *1*, 2020−2024.
(22) Nandy, B.; Maiti, P. K.; Bunker, A. *J. Chem. Theor. Comput.* **2012**, *9*, 722−729.
(23) Cakara, D.; Kleimann, J.; Borkovec, M. *Macromolecules* **2003**, *36*, 4201−4207.
(24) Kukowska-Latallo, J. F.; Bielinska, A. U.; Johnson, J.; Spindler, R.; Tomalia, D. A.; Baker, J. R. *Proc. Natl. Acad. Sci. U.S.A.* **1996**, *93*, 4897−4902.
(25) Morille, M.; Passirani, C.; Vonarbourg, A.; Clavreul, A.; Benoit, J. P. *Biomaterials* **2008**, *29*, 3477−3496.
(26) Peng, S. F.; Su, C. J.; Wei, M. C.; Chen, C. Y.; Liao, Z. X.; Lee, P. W.; Chen, H. L.; Sung, H. W. *Biomaterials* **2010**, *31*, 5660−5670.
(27) Su, C. J.; Chen, C. Y.; Lin, M. C.; Chen, H. L.; Iwase, H.; Koizumi, S.; Hashimoto, T. *Macromolecules* **2012**, *45*, 5208−5217.
(28) Su, C. J.; Chen, C. Y.; Chen, H. L.; Ivanov, V. A. *J. Phys. Conf. Ser.* **2011**, *272*, 012002.
(29) Evans, H. M.; Ahmad, A.; Ewert, K.; Pfohl, T.; Martin-Herranz, A.; Bruinsma, R. F.; Safinya, C. R. *Phys. Rev. Lett.* **2003**, *91*, 075501.
(30) Zhou, S. Q.; Liang, D. H.; Burger, C.; Yeh, F. J.; Chu, B. *Biomacromolecules* **2004**, *5*, 1256−1261.
(31) Liu, Y. C.; Chen, H. L.; Su, C. J.; Lin, H. K.; Liu, W. L.; Jeng, U. S. *Macromolecules* **2005**, *38*, 9434−9440.
(32) Ewert, K. K.; Evans, H. M.; Zidovska, A.; Bouxsein, N. F.; Ahmad, A.; Safinya, C. R. *J. Am. Chem. Soc.* **2006**, *128*, 3998−4006.
(33) Su, C. J.; Chen, H. L.; Wei, M. C.; Peng, S. F.; Sung, H. W.; Ivanov, V. A. *Biomacromolecules* **2009**, *10*, 773−783.
(34) Dootz, R.; Toma, A. C.; Pfohl, T. *Soft Matter* **2011**, *7*, 8343−8351.
(35) Chen, C. Y.; Su, C. J.; Peng, S. F.; Chen, H. L.; Sung, H. W. *Soft Matter* **2011**, *7*, 61−63.
(36) Carnerup, A. M.; Ainalem, M. L.; Alfredsson, V.; Nylander, T. *Soft Matter* **2011**, *7*, 760−768.
(37) Ainalem, M. L.; Nylander, T. *Soft Matter* **2011**, *7*, 4577−4594.
(38) Stryer, L. *Biochemistry*; W. H. Freeman and Company: San Francisco, CA, 1981.
(39) Widom, J. *Annu. Rev. Biophys. Biomol. Struct.* **1998**, *27*, 285−327.
(40) Debye, P. *Ann. Physik.* **1915**, *46*, 809−823.
(41) Porcar, L.; Hong, K. L.; Butler, P. D.; Herwig, K. W.; Smith, G. S.; Liu, Y.; Chen, W. R. *J. Phys. Chem. B* **2010**, *114*, 1751−1756.
(42) Hamley, I. W. *Macromolecules* **2008**, *41*, 8948−8950.
(43) Ray, J.; Manning, G. S. *Macromolecules* **1999**, *32*, 4588−4595.
(44) Fenley, M. O.; Olson, W. K.; Manning, G. S. *Macromolecules* **2000**, *33*, 1899−1903.
(45) Manning, G. S. *Macromolecules* **2007**, *40*, 8071−8081.